Petroleum and Coal

Prediction of Spatial Variability in Grain Size Distribution on Outcrop from Gamma Ray Measurement

Amirah Khairiyah Johari, Bashir Busahmin*, Stephen Tyson

Petroleum and Chemical Engineering, Universiti Teknologi Brunei, Brunei Darussalam

Abstract

The total gamma values and the three radioactive mineral values recorded by sophisticated tool where the correlation between them was measured. Grain size analyses were performed using the Sieve Shaker to calculate the mass retained, the mean grain size and the sediment type for each of the rock extracted. The use of RS-332 SGR equipment revealed the cross plotting radioactive minerals. This paper highlights the use of Spectral Gamma Ray (SGR) RS-332 tools to analyze rock lithology, grain sizes and the geological analysis of the outcrop. In addition, the cumulative and probability distribution of Brunei region were computed to describe the grain size distribution and sediment type. Moreover, fine sand sediment type concluded that more of the rock samples collected were montmorillonite. The main objective of this paper is to study the spatial distribution pattern of the grain size and their correlation to naturally occurring radioactive minerals which include potassium, uranium, and thorium., Furthermore, python software is used to create spatial variability by interpolation, choosing kriging method for reliable variability results.

Keywords: Grain size; Python; Correlation; Lithology; Radioactive minerals; Spectral gamma ray.

1. Introduction

Borneo, the third-largest island in the world, is encircled by sedimentary basins that are very hydrocarbon-rich and these basins were formed because of Borneo's elevation during the Neogene era where the river deltas grow farther out into the sea that resulted in the deposition of a thick succession of sediments, in addition, sediments were deposited in the north and east of Borneo due to the uplift movement at the Centre of Borneo mountains [1]. The heterogeneity or the differences in values or features of the phenomenon across the specific geographic area are referred to as spatial variability [2]. When analyzing petroleum outcrops, spatial variability is crucial to be considered since it can provide the key details about the subsurface geology and probable reservoir characteristics, moreover, the depositional conditions and the sediments transport is indicated by the spatial changes in grain size and sorting [3]. Additionally, porosity and permeability of the reservoir rock is influenced by the spatial distribution of minerals, such as clay minerals and feldspars [4]. Grain size distribution patterns spatial patterns may be related to the environmental factors such as transport mechanisms, hydrodynamics, and sediment origins [5]. The distribution of silt and clay fractions are higher in the upstream area and lower in the seaward region, additionally, Brunei estuary was mostly made up of sand fractions and the study demonstrated that the organic matter in sediments interacted closely with the smaller fractions of the sediment like silt and clay, however, and due to the sand-silt-clay mixing in the inner estuary, which is regulated by the bidirectional tidal fluxes, where there is a significant sediment exchange [6]. Moreover, the cross-validation analysis is used to assess the performance of the experimental variogram model once it has been produced. In cross-validation, the data was split into training and validation sets, the variogram model was fitted to the training set, and the model was used to interpolate the values at the validation set locations, and the model was deemed suitable and maybe used

for kriging procedure when successfully the values predicted at the locations in the validation set [7-8]. Furthermore, an estimation or the cross-validation error calculated by deducting each measured value from its estimated value, resulting in an error distribution for the entire dataset. However, there are multiple ways to estimate the errors, for example the mean standardized error (MSE), the root means square standardized (RMSEE), and the correlation coefficient after Spearman (CS). MSE is at its best when equals to zero. RMSEE is ideal when the ratio of mean squared cross-validation errors and the kriging variances is equal to one. CS is equal to one when the correlation is ideal, and it is equal to zero when there is no correlation [9]. Reservoir properties are highly influenced by clay content where clay mineral limits the pathway of fluid transmission inside the rock, and it also fills up the empty voids which decreases the rocks porosity; thus, clay content was evaluated from the individual concentrations data of the mineral which are thorium, uranium, and potassium [10]. When the Th/U ratio is lower than two (Th/U < 2), there is a high possibility that it is a reducing condition and when the Th/U ratio is greater than seven (Th/U > 7), there is a high probability that is it an oxidizing condition [11]. Moreover, the high gamma ray value of shales is due to the abundant presence of potassium unlike in other sedimentary rocks, namely sandstone, limestone, coal, salt, and carbonate. Therefore, potassium is the typical component found in clay content due to the cation exchangeability of clay minerals that absorbs uranium and thorium elements [12].

$$GR = 16.5\,K + 7.48U + 4Th \tag{1}$$

whereas: GR is gamma ray [API]; U, Th, K – rock content of U [ppm]; thorium Th [ppm]; potassium K [%].

Grain size also is called particle size and is the diameter of the individual grains of sediment. In addition, grain size analysis is a standard experimentation to derive the particle size distribution within the rock to understand geology for petroleum reservoir, and the measurement of particle size helps in drilling fluid formulation to assess proficient drilling operations elements and predicts the well performance using Taylor series [13-14]. Moreover, the grain-size distribution curve is used to calculate the values for D10, D30, and D60, which are the diameters that correspond to the percent finer of 10%, 30%, and 60%, respectively, equations 2 and 3 are used to obtain the uniformity coefficient (C_u) and the coefficient of gradation (C_c) values:

$$C_c = \frac{(D_{30})^2}{D_{60} \times D_{10}} \tag{2}$$

$$C_u = \frac{D_{60}}{D_{10}} \tag{3}$$

The classification of whether the soil is well-graded or not is based on the values of C_u and C_c. When C_u is larger than 6 and Cc is between 1 and 3, then sand is well-graded. Gravel should have a C_u value more than 4 and C_c value is between 1 and 3 to be deemed well-graded. The main objective of this paper is to study the spatial distribution pattern of the grain size and their correlation to naturally occurring radioactive minerals which include potassium, uranium, and thorium. Moreover, Python software is used to create spatial variability by interpolation, choosing kriging method for reliable variability results.

2. Methodology

2.1. Location of study

This paper focuses on one outcrop that is located along Jalan Tutong (4°45'59.6"N, 114°44'41.1"E) in Brunei, which exposes to a sedimentary deposit from the Miri and Seria formations. In Brunei, outcrops of the Seria formation are along the coastlines of the Tutong and Belait Districts where it was deposited during the late Miocene. In addition, the selection of the outcrop was based on accessibility, exposure, diversity, and relevancy of this research work. Therefore, the sedimentary strata are clear, distinct, and the outcrop is well exposed. To produce the spatial variability of the grain size in Brunei, Gamma Ray Spectrometer (GRS) RS-332 as shown in Figure 1.

RS-332 SGR

Holding the RS-332 for 3 minutes for assay data collection.

Jalan Lamunin Outcrop

Rock Extracted

Jalan Lamunin 3D Outcrop (Photogrammetry)

Outcrop bedding division
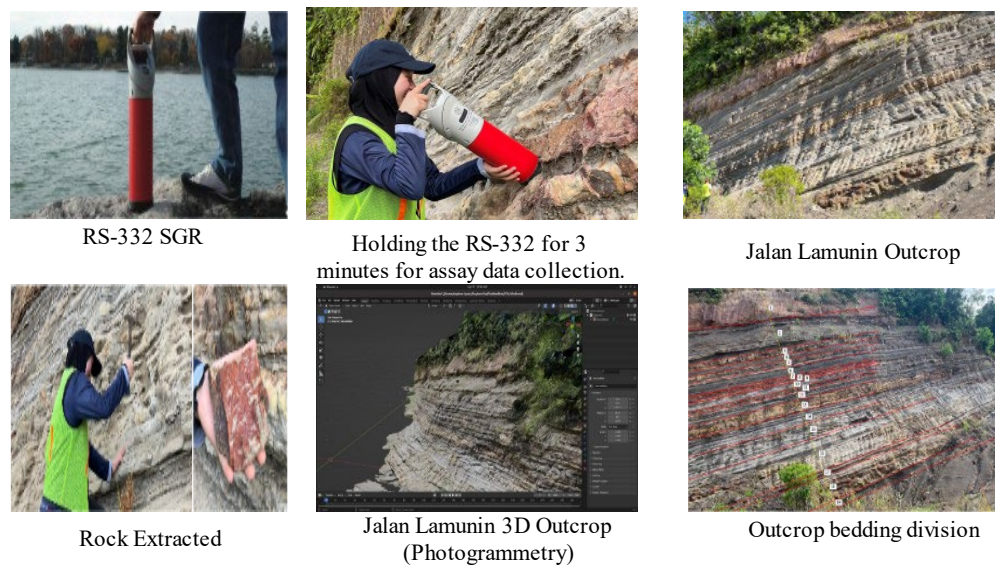
Figure 1. Jalan Lamunin Outcrop (Brunei Darussalam).

2.2. Tools used

Sieve shaker is required to measure the grain sizes and the characterizes stratigraphic boundaries indicated that low gamma-ray values mean a coarse grain size while high gamma-ray values represented a finer grain size, in addition, a laptop was required to install RS Analyst to create the database, then the data were transferred to Python programming software. Moreover, pickaxe was used to break up the rocks into grain sizes. Besides, clear zip lock bags and marker pens were used to place the samples labeled to avoid any misinterpretation during the data gathering, other tools were used like geology hammer, compass clinometer, hand lens, 50 tape meter, mechanical pencils, refills and erasers, notebook, sedimentary grain size card, graphic log sheets, sample bags, permanent marker/sharpie, and boxes. Furthermore, the detector is made up of three by 3-inch sodium-iodide (NaI) that enhances the tools sensitivity in detecting the electromagnetic radiation emission by the elements and the color screen changes into a monochrome screen in strong sunlight easing the reading. IP65 weatherproofing is included to protect against any immersion like water or any rock debris. Likewise, the system was stabilized to remove any flawed effects to obtain an accurate result.

2.3. Modes of operation and data storage

RS-332 has four modes of operation which are Assay, Survey, Identity and Spectrum. The Assay mode shows the values of potassium-40 (K), uranium (U), thorium-232 (Th), Dose and Dose Rate. In addition, the distribution of K, U and Th may provide information like the genesis of rocks. Furthermore, the type of clay minerals, the depositional environment and the total organic matter were evaluated by cross plotting the isotopes, hence the survey mode presented the radiation level detected by the system. RS-332 that has five main menus which are the Settings, Data Storage, Assay, Survey, and Shutdown. The system was equipped with a solid-state memory drive where the extracted data was saved. Once the rock samples have been collected, placed in plastic bags marked with an assay ID number for easy reference, also it is important to note that the size of the rock sample must be equivalent to the size of a fist, because is necessary to ensure that each sample collected weighs be at least 100 g, and that is the minimum required weight for sieve analysis. In addition, by maintaining the consistency in the collection of rock samples and conducting an accurate grain size analysis, reliable data are obtained, aiding in the successful interpretation and correlation of the assay data with the radioactive minerals.

2.4. Outcome of assay data

The ratio of thorium and potassium is an indicative of the clay minerals, while the ratio of thorium and uranium reveals the depositional setting. Python software was used to create boxplots of the ratios of radioactive minerals and error bars.

3. Results and discussion

3.1. Gamma total Log

Gamma total log is displayed as a continuous curve at various depths of the outcrop as shown in Figure 2, on the first left side of the Figure 2 is the result of the log of the gamma integral, when the latitude of the measurement file in meters is used as the distance, in addition, the y-axis distance (m) does not represent the actual height of the outcrop, which is 14.95 m. The second gamma total from the left presented the average gamma total for each bed, as a result, the cumulative distance of the bed is placed as the distance values in the survey file.
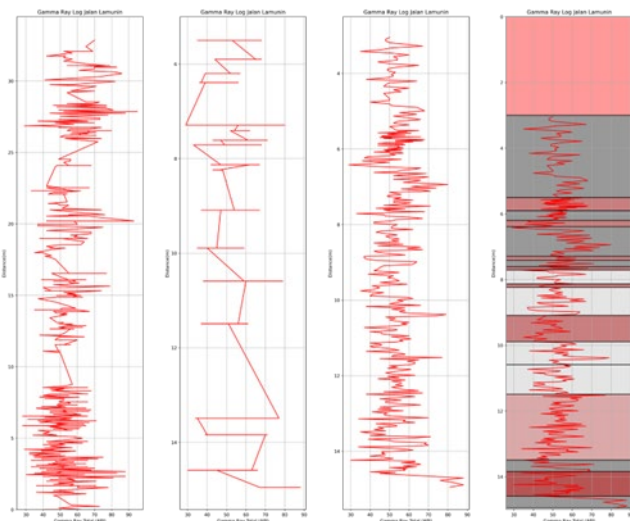
Figure 2. Gamma total Log.

The highest gamma total eighty-eight was recorded in bed nineteen, and the lowest gamma total is twenty-nine which was recorded in bed 6. Moreover, Bed 2 is on the top and follows bed nineteen on the bottom of the log. The third log from the left represents the correct gamma total log because the cumulative distance is calculated from the incremental increase in the thickness of the outcrop. Thus, the incremental increase is calculated by dividing the bed thickness by the total number of survey data while the cumulative thickness is calculated by adding the incremental increase for each data point with the previous cumulative distance value. The far right of Figure 2 shows the gamma total log with its corresponding lithology for each bed.

3.2. Sieve shaker

Figure 3 shows the cumulative data according to the assay values and are grouped into intervals of ten units each.
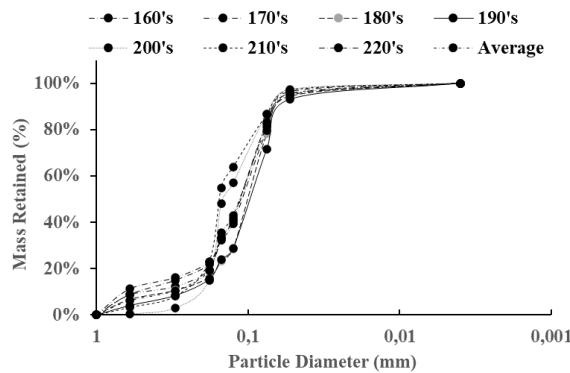
Figure 3. Cumulative distribution for mass retained versus particle size.

Figure 4 shows the probability distribution according to the bed, the cumulative distribution showed a hump, and the probability distribution showed 2 and 3 peaks which indicated a bimodal and trimodal distributions, respectively. In addition, the probability distribution presented the 3 highest peaks at 23.44% mass retained of 0.6 mm particle diameter (coarse sand) which belongs to bed 2, at 49.95% mass retained of 0.15 mm particle diameter (fine sand) that belonged to bed 15, at 64.83% mass retained of 0.075 mm particle diameter (very fine sand) belonged to bed 1, however, this distribution has given a biased interpretation of beds that have many grain data, moreover, bed 18 has the most grain data with 23-grain data followed by 8-grain data for bed 16. Furthermore, other beds have 2-grain data except for bed 1 and bed 3 with one-grain data, despite that, the distributions provided the information on the particle characteristic size of the sample, mean particle size, mode, the most common particle size, and the standard deviation.
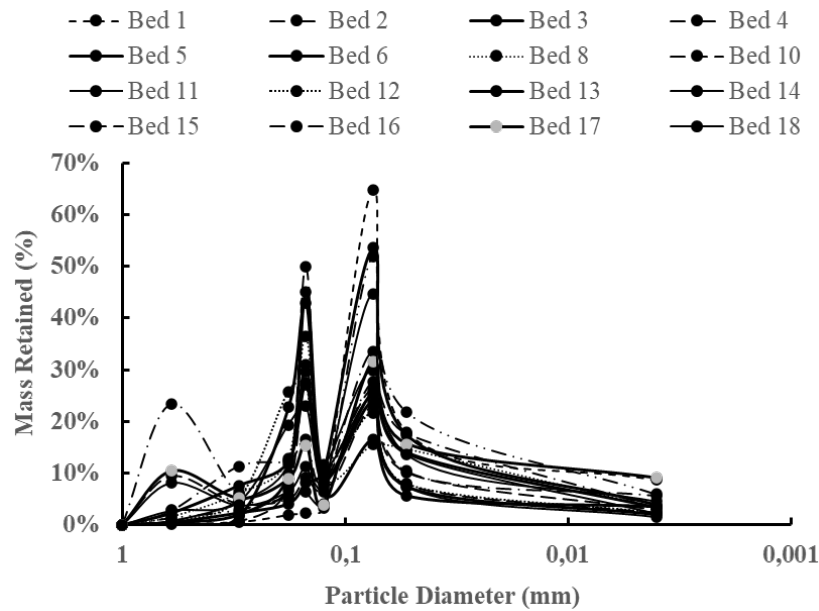
Figure 4. Probability distribution.

Table 1. Sediment type for each rock sample.

Bed unit	Assay ID	Sediment type	Bed unit	Assay ID	Sediment type
1	226	Very fine sand	16	199	Very fine sand
2	224	Very fine sand	16	200	Very fine sand
2	225	Very fine sand	16	201	Very fine sand
3	222	Very fine sand	17	195	Very fine sand
3	223	Not enough weight	17	196	Very fine sand
4	220	Very fine sand	18	166	Fine sand
4	221	Very fine sand	18	167	Very fine sand
5	218	Fine sand	18	168	Very fine sand
5	219	Fine sand	18	169	Very fine sand
6	216	Very fine sand	18	170	Very fine sand
6	217	Fine sand	18	171	Very fine sand
8	214	Fine sand	18	172	Very fine sand
8	215	Fine sand	18	173	Very fine sand
10	212	Fine sand	18	174	Very fine sand
10	213	Fine sand	18	175	Very fine sand
11	210	Very fine sand	18	176	Very fine sand
11	211	Very fine sand	18	177	Very fine sand
12	208	Fine sand	18	178	Very fine sand
12	209	Fine sand	18	179	Very fine sand

Bed unit	Assay ID	Sediment type	Bed unit	Assay ID	Sediment type
13	206	Fine sand	18	180	Very fine sand
13	207	Fine sand	18	181	Very fine sand
14	204	Fine sand	18	182	Very fine sand
14	205	Fine sand	18	183	Very fine sand
15	202	Fine sand	18	184	Very fine sand
15	203	Fine sand	18	185	Very fine sand
16	188	Very fine sand	18	186	Missing
16	189	Very fine sand	18	187	Very fine sand
16	190	Very fine sand	18	194	Very fine sand
16	197	Very fine sand	16	198	Very fine sand
19	193	Not enough weight			

3.3. Correlation

A positive correlation coefficient (represented by values between 0 and +1) indicated that as one variable increased, the other variable also tends to increase. A negative correlation coefficient (represented by values between 0 and -1) indicated that as one variable increased, the other variable tends to decrease as well. In addition, it is significant to note that a correlation coefficient only indicates the strength and the direction of the relationship between the two variables but does not provide information on causality. Figure 5 shows the correlation coefficient between the three radioactive minerals with clay content. Furthermore, the correlation coefficients are -0.01, 0.33, 0.21 for potassium, uranium, and thorium respectively and all the three-correlation coefficients showed a weak correlation as the values were closer to 0 than 1 or -1, moreover, the clay content ranged from 7.38 % to 41.23 %. Hence, clay content and potassium showed the weakest correlation because it is closer to 0 when to compare it with the other two correlations, and the only the correlation for clay content and potassium showed a negative value that means as clay content increased.
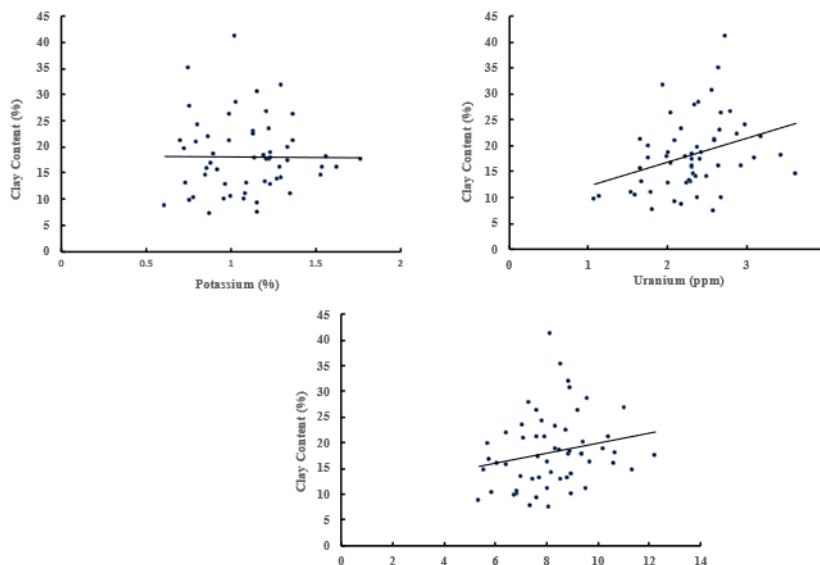
Figure 5. Correlation between clay content (%) and radioactive minerals.

Figure 6 shows the correlation coefficient between the three radioactive minerals with the mean grain size, as a result the correlation coefficients are 0.16, -0.27, and 0.01 for potassium, uranium, and thorium, respectively. All three-correlation coefficients showed a weak correlation as the values are closer to 0 than 1 or -1. In addition, the correlation between the mean grain size and thorium showed the weakest correlation as it is closer to 0 compared to the other two correlations. Figure 7 shows the correlation coefficient between the API values with the mean grain size. The correlation coefficient is -0.02 and the correlation coefficient is

close to 0, it indicated that there is no linear relationship between the mean grain size and API hence, the relationship is weak. Moreover, the API values ranged from 45.05 to 111.20 and the mean grain size ranged from 0.086 mm to 0.170 mm.
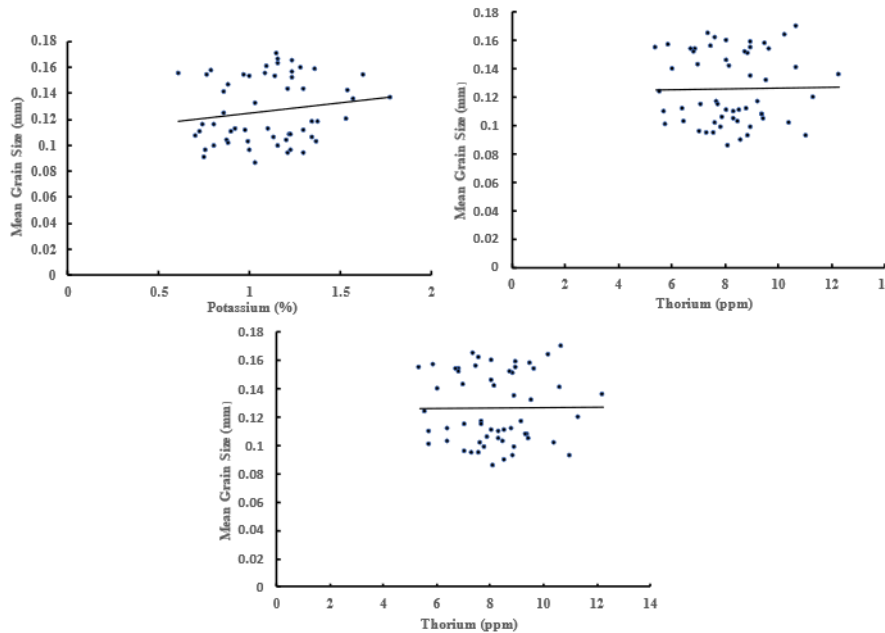
Figure 6. Correlation between mean grain size (mm) and radioactive minerals.
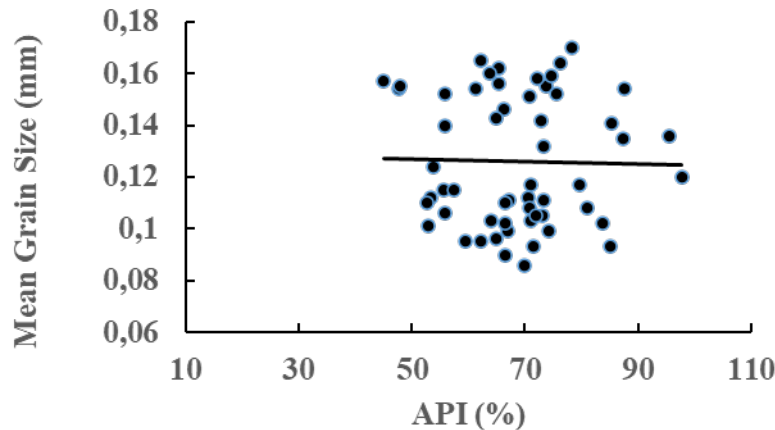
Figure 7. Correlation between mean grain size (mm) and the API.

3.4. Spatial interpolation

Figure 8 presents linear and cubic interpolation, where using linear interpolation, it showed that potassium has lower values in the Centre and increased outward and the spatial shapes are triangles and rectangles. In addition, the upper right side has higher potassium values compared to the rest of the area with higher values at the bottom right. Moreover, many areas are covered with values from 0.80 % to 1.40 %. Studying cubic interpolation, the spatial is more distributed in an ellipse and circular shapes and the values ranged from 0 % to 2.4 %, however, there are negative values on the extreme left and this is due to no data recorded on those areas. Figure 9 presents the grain size values increased from top to bottom, and it decreased at the end. The interpolated area with purple color indicated a high value due to holding more grain size in the region where the values ranged from 0.15 mm to 0.17 mm. Investigating the cubic interpolation, the spatial was more largely covered with a certain range of values hence more colored area, unlike the linear interpolation where the color gradient

changes rapidly. On the other left side, it showed a negative value due to lack of data collected in the regions.
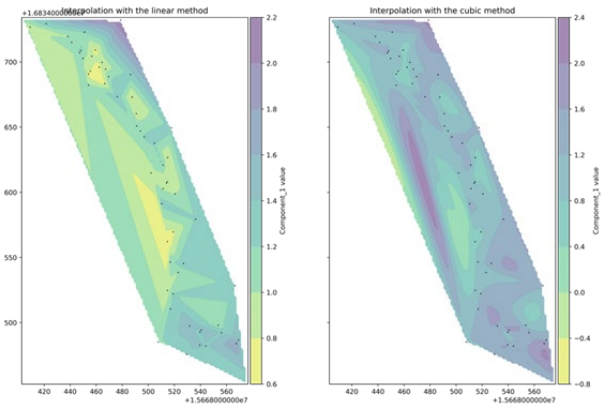
Figure 8. Linear and cubic interpolation of potasium.
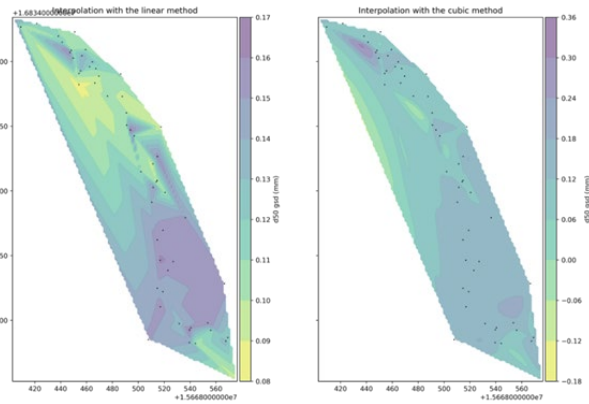
Figure 9. Linear and cubic interpolation of grain size distribution.

3.5. Ordinary kriging and error estimation

Figure 10 shows the ordinary kriging estimation for potassium and its error. The ordinary kriging presented initially a lower value in the Centre left, then increased outward towards the top and the bottom right corner, while the error has a lower value in the Centre, and it increased outward hence the lighter yellow color surrounding the area. In addition, Grain size ordinary kriging estimation [15] and its error was shown in Figure 11 where the top area has lower ordinary kriging estimation values and the bottom area has larger estimation values. Moreover, as for its error, it is the same as potassium where the Centre has lower values, and it increased outward.
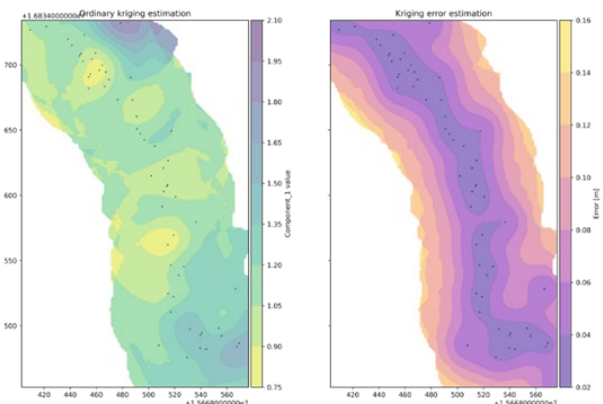
Figure 10. Potassium ordinary kriging and its error.
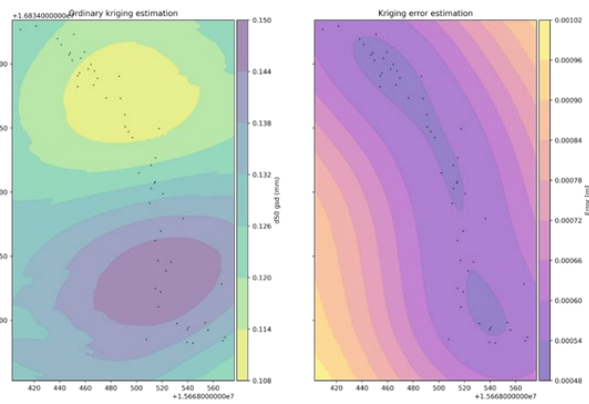
Figure 11. Grain size ordinary kriging and its error.

4. Conclusions

The investigation of the outcrop in Brunei Darussalam was conducted to provide the spatial variability of grain size distribution. The data obtained from Spectral Gamma Ray RS-332 and sieve shaker was combined using Python software to deliver the outcrop lithology, sediment types, depositional settings, clay mineralogy, and gamma total log, the outcrop and sieve analysis were based on the rock samples, in addition, the outcrops had a total of 19 beds with a height of 14.95 m, and 62 rocks. The Th/K cross-plot showed montmorillonite mineral with two mixed layers. Moreover, from the Th/U cross-plot, it was concluded that the depositional environment is in the shallow marine and the sediments were grey and green shales. Therefore, the maximum error obtained using SGR RS-332 for potassium, uranium and thorium values were 4.61%, 9.87% and 7.13% respectively for the sieving error, the average sieving

error was 0.19% and that is good because the error is minor. The gamma total log displayed a continuous curve at different depths ranging from 29 to 88 resulting from bed 6 and bed 19. The cumulative distributions of mass retained showed 2 and 3 peaks which indicated a bimodal and trimodal grain size distributions, however, the cumulative distribution does not show the actual individual rock sample distribution.

References

[1] Baillie SR, Doherty PF. Analysis using large-scale ringing data. Animal Biodiversity and Conservation, 2004; 27(1).

[2] Li J, Li X. Spatial Variability. Encyclopedia of Ocean Engineering. Springer, Singapore,2021. https://doi.org/10.1007/978-981-10-6963-5_214-1 .

[3] van Hateren JA, van Buuren U, Arens SM, van Balen RT, and Prins MA. Identifying sediment transport mechanisms from grain size–shape distributions, applied to aeolian sediments. Earth Surf. Dynam., 2020; 8: 527–553, https://doi.org/10.5194/esurf-8-527-2020,2020

[4] Risha M, Tsegab H, Rahmani, O, Douraghi J. The Impact of Clay Minerals on the Porosity Distribution of Clastic Reservoirs: A Case Study from the Labuan Island, Malaysia. Appl. Sci. 2023; 13: 3427. https://doi.org/10.3390/app13063427

[5] Maillet GM, Vella C, Durand M, Mojtahid M. Spatial variability of surface sediments grain-size of the Loire Estuary. Conference: 33rd IAS & 16th ASF International Meeting of Sedimentology, 2017.

[6] Hossain MB, Marshall DJ, Senapathi V. Sediment granulometry and organic matter content in the intertidal zone of the Sungai Brunei estuarine system. Carpathian Journal of Earth and Environmental Sciences, 2014; 9(2):231-239.

[7] Jerosch K. Geostatistical mapping and spatial variability of surficial sediment types on the Beaufort Shelf based on grain size data. Journal of Marine Systems, 2013; 127:5–13. https://doi.org/10.1016/j.jmarsys.2012.02.013

[8] Kim A, Busahmin B, Tyson S. Compositional Kriging Analysis: A Spatial Interpolation Method for Distribution. ARPN Journal of Engineering and Applied Sciences, 2024; 19(1): 9–15.

[9] Pesch R, Pehlke H, Jerosch K, Schröder W, Schlüter M. Using decision trees to predict benthic communities within and near the German Exclusive Economic Zone (EEZ) of the North Sea. Environmental Monitoring and Assessment, 2008; 136(1-3):313-25. https://doi.org/10.1007/s10661-007-9687-1

[10] Klaja J, Dudek L. Geological interpretation of spectral gamma ray (SGR) logging in selected boreholes. NaftaGaz, 2016; 72(1): 3-14.

[11] Vigh T, Kovács T, Somlai J, Kávási N, Polgári M, Bíró L. Terrestrial Radioisotopes in Black Shale Hosted Mn-Carbonate Deposit (Úrkút, Hungary). Acta Geophysica, 2013; 61(4): 831–847. https://doi.org/10.2478/s11600-013-0124-2

[12] Ibrahim WE, Salim AMA, Sum CW. Mineralogical investigation of fine clastic rocks from Central Sarawak, Malaysia. Journal of Petroleum Exploration and Production Technology, 2019; 10(2):21-30. http://doi.org/10.1007/s13202-019-00751-0

[13] Jo HJ, Hong SH, Lee BM, Kim YJ, Hwang WR, Kim SY. High energy dissipation-based process to improve the rheological properties of bentonite drilling muds by reducing the particle size. Ultrasonics Sonochemistry, 2022; 92(3-4):106246, https://doi.org/10.1016/j.ultsonch.2022.106246

[14] Okologume WC, Omonusi R. Determination of Well Performance for Gas Wells: A Novel Prediction Method Using Taylor Series. Petroleum and Coal, 2023; 65(1): 260-266.

[15] Kim A, Busahmin B, Tyson S. Prediction of Grain Size Distribution Using Ordinary Kriging and Compositional Kriging Methods. ARPN Journal of Engineering and Applied Sciences. 2024, 19(9): 556–562

To whom correspondence should be addressed: , Bashir Busahmin, Petroleum and Chemical Engineering, Universiti Teknologi Brunei, Brunei Darussalam, E-mail: bashir.abusahmin@utb.edu.bn